

The role of CENPO expression in the progression of non-small cell lung cancer

Yanlong Yang

Kunming Medical University First Affiliated Hospital <https://orcid.org/0000-0002-9512-3956>

Xiaobo Chen

Kunming Medical University First Affiliated Hospital

Hongwen Sun

Kunming Medical University First Affiliated Hospital

Qinghe Yu

Kunming Medical University First Affiliated Hospital

Fang Yin

Kunming Medical University First Affiliated Hospital

Zaoxiu Hu

Yunnan Cancer Hospital

Yongmeng Sun

Kunming Medical University First Affiliated Hospital

Lisha Pu

Kunming Medical University

Xinming Zhu

Kunming Medical University First Affiliated Hospital

Shen Li

Kunming Medical University

Yunping Zhao (✉ zhaoypcq@126.com)

<https://orcid.org/0000-0001-8932-9440>

Primary research

Keywords: Centromere protein O, non-small cell lung cancer, progression

Posted Date: September 3rd, 2020

DOI: <https://doi.org/10.21203/rs.3.rs-55345/v2>

License:   This work is licensed under a Creative Commons Attribution 4.0 International License.

[Read Full License](#)

Abstract

Background: The role of Centromere protein O (CENPO) in the development of non-small cell lung cancer (NSCLC) is unknown. This study aimed to investigate the potential role of CENPO in the development of NSCLC.

Methods: The expression level of CENPO was investigated in both tissues and cell-lines. Cell counting assay, wound-healing assay, Transwell assay and Flow cytometry was used to explore the effect of CENPO on proliferation, migration, invasion, apoptosis and cell cycle of NSCLC. The potential mechanism of CENPO was explored by Human Apoptosis Antibody, also, western blot was conducted to detect the expression of PI3K/Akt/mTOR pathway and cell-cycle related protein (mTOR, P-mTOR, CDK1, CDK6 and PIK3CA). Besides, the effect of CENPO on the growth of NSCLC solid tumors was demonstrated in vivo.

Results: Our study suggested CENPO gene overexpression in NSCLC. Reduced CENPO expression substantially decreased the proliferation, migration and invasion ability, and promoting apoptosis and induces cell cycle arrest of NSCLC cell-lines. Preliminary mechanism research suggested reduced CENPO could active apoptosis pathway, suppressing PI3K/AKT/mTOR pathway and down-regulation cell-cycle related proteins.

Conclusion: CENPO was up-regulated in NSCLC and played an important role in promoting the progress of NSCLC.

Introduction

The morbidity and mortality of lung cancer was the highest worldwide, with 2.1 million new lung cancer cases and 1.8 million deaths in 2018, representing close to 1 in 5 (18.4%) cancer deaths based on the GLOBOCAN 2018.(1) In China, lung cancer was also still a fatal threat to people's health, with the incidence of 774,323 and the mortality of 690,567 in 2018.(2) Non-small cell lung cancers (NSCLCs) account for approximately 85% lung cancer cases, which could be divided into 2 major types - lung adenocarcinoma (LUAD) and lung squamous cell carcinoma (LUSC).(3) Nowadays it is accepted that LUAD is the dominant subtype, especially in Asian women (more than 70% in Japanese females). Although many advances have been made in the early detection and treatment of lung cancer, the prognosis remains poor, with an overall 5-year survival rate ranging from 15% to 20%. Recently, many targetable gene alterations have been identified to benefit from targeted therapy and immunotherapy, however, not all lung cancer have targetable gene alterations, and many patients develop resistance to targeted therapy. The heterogeneity was a major problem and a challenge for lung cancer treatment. The reason for this heterogeneity might be the difference in molecular features and biological behaviors among lung cancers. With the development in molecular biology, for example, the use of next-generation sequencing, we could make it possible in understanding the distinct molecular feature in lung cancer.

Correct transmission of genetic material during the chromosome segregation in cell division is critical for the survival of cells. Errors in chromosome segregation may result in some genetic disease, also neoplasia. The formation of kinetochore is essential in the process of chromosome segregation. (4) Recent studies have demonstrated that kinetochore is a macromolecular complex consisted of many proteins. The kinetochore protein complex can be roughly divided into constitutive centromere-associated network (CCAN) and KMN (KNL1-Mis12 complex-Ndc80 complex) network. (5) CCAN constitutively localizes to centromeres throughout the cell cycle, and KMN targeted into CCAN during late G2 to establish the complete kinetochore structure in mitosis. (6) CCAN is comprised by centromere proteins. Generally, these proteins could be classified as several functional groups: CENP-C, CENP-H/I/K/M, CENP-L/M, CENP-O/P/Q/R/U, CENP-T/W and CENP-S/X. (5) Aberrant expression of centromere proteins would cause cancers. CENP-A, CENP-M, CENP-U/50, CENP-W, CENP-H and CENP-R were over-expressed in some cancers and were associated with poor prognosis.

In our current study, we focused on centromere protein O (CENPO), which formed CENP-O/P/Q/U complex. Previous study showed CENP-O/P/Q/R/U-deficient chicken DT40 cells are viable, but show defects during the process of recovery from spindle damage (7). Depletion of CENPO proteins by siRNA frequently induced aneuploidy in RKO cells. Accumulation of aneuploid chromosomes would lead to the development of cancer. (8) The researches about the role of CENPO and the potential mechanism in cancer were limited. Only Cao Y et al reported that CENPO was upregulated in gastric cancer and was associated with poor survival. Reduced CENPO contributed to cell growth inhibition and apoptosis induction. (9) Further studies were needed to validate the role of CENPO in other cancers and explore its potential role.

In the current study, we comprehensively investigated the role of CENPO expression in the progression of NSCLC. Firstly, we examined the expression level of CENPO in NSCLC tissues and cells. Secondly, we explored the role of CENPO in proliferation, migration, invasion, apoptosis and cell cycle on NSCLC by both using cell-line and orthotopic xenograft models. Finally the preliminary mechanism of CENPO in the tumorigenesis of NSCLC was investigated.

Materials And Methods

Clinical samples and cell culture

The tissue microarray consisting 75 NSCLC tissues and 51 adjacent normal lung tissues were obtained from Shanghai Outdo Biotech Co., Ltd (HLug-Squ150Sur-02, Shanghai, China).

Human NSCLC cell-lines A549, NCI-H1299, SPC-A-1 and normal lung epithelial cell line EBC-1 were purchased from American Type Culture Collection (ATCC, Manassas, VA, USA). The cells were cultured in RPMI-1640 (Corning Company, NY, USA) with 10% fetal bovine serum (FBS, Ausbian, Vian-Saga Biotechnology Co., Ltd, Shanghai, China) in moist air containing 5% CO₂ at 37°C.

Bioinformatics analysis

The transcriptional level of CENPO between cancerous and paired normal tissues and its relationship between clinicopathologic features was analyzed by online UALCAN (<http://ualcan.path.uab.edu/>) which based on TCGA database.(10) The prognostic role of CENPO on LUAD and LUSC was explored by Kaplan-Meier Plotter (KM Plotter, <http://kmplot.com/analysis/>).(11)

Immunohistochemical (IHC) staining

The paraffin sections were dewaxed in xylene, and then Antigen Retrieval Buffer (Maixin biotechnology co. LTD, Fuzhou, China). The sections were washed 3 times with 1 × PBST for 5 min each time. 3% H₂O₂ was used for sealing the endogenous peroxidase of tissues. Then sections were incubated with primary antibodies (anti-CENPO 1:50, biorbyt), Ki67 (1:200, abcam) overnight at 4°C. After being washed, the sections were incubated with second antibody IgG H&L (HRP) (1:400, abcam) overnight at 4°C. The sections were stained with DAB and then counterstained with hematoxylin (Baso Diagnostics Inc., Zhuhai, China). Absolute ethanol was used to dehydrate the sections and then neutral resin (China National Pharmaceutical Group Co., Ltd, Beijing, China) was used to seal the sections. Based on the proportion of positive cells and the intensity of staining, a scoring system was used to determine the expression level of CENPO. The percentages of positively stained cells were scored as follows: 0 (0%), 1 (1-25%), 2 (25-50%), 3 (50-75%) and 4 (≥75%). The signal intensity was analyzed as follows: 0 (negative), 1 (weak), 2 (moderate), and 3 (strong). A final score was calculated by multiplying the percentage and signal intensity scores. The specimen with final score >2 were considered as high CENPO expression, otherwise were regarded as low.

Real-time quantitative PCR (qRT-PCR)

Total RNA was extracted from cells using Trizol reagent (sigma), then RNA was reverse transcribed into cDNA by Hiscript QRT supermix for qPCR (+gDNA WIPER) (vazyme) according to manufacturer's instruction. Two-step Real time PCR was applied. The primer sequences for qRT-PCR were as following: CENPO forward, 5'-TGCTTTTGAGGGGAACCTATTG-3' and reverse, 5'-GGGGAATGAAGACTGGGACT-3'; GAPDH forward 5'-TGA CTTC AACAGCGACACCCA -3' and reverse, 5'-CACCTGTTGCTGTAGCCAAA-3'. Total PCR system was 10 μL. The relative expression level of CENPO was calculated using the $2^{-\Delta\Delta C_t}$ method. (12)

Western blot

The protein were extracted from cells by 1 × Lysis buffer, then the concentration was measured by BCA Protein Assay Kit (Cat 23225, Hyclone-Pierce). 10% SDS-PAGE was used to separate protein and then the proteins were transferred to PVDF membrane. The membrane was blocked with 1 × TBST solution with 5% skimmed milk for 1 h at room temperature and then incubated at 4°C overnight with primary antibodies. After that, the membrane was incubated with secondary antibodies at room temperature for 2 h. At last, immobilized western Chemiluminescent HRP Substrate was used to visualize the protein expression level.

Lentivirus RNAi construction and infection

Oligonucleotides for small hairpin RNAs (shRNAs) targeting the CENPO were designed (shRNA1: 5'-AGAAGCATTGGAAGAGAAATT-3', shRNA2:5'-GCAGAGAAACCCACTGTGTAA-3', and shRNA3:5'-CCTGGAAGAGATAGCTGCAAA-3'). The control shRNA sequence was 5'-TTCTCCGAACGTGTCACGT-3'. These pairs of oligonucleotides were annealed and cloned into BR-V108 Vector. The generated plasmids were cotransfected into 293T cells using lipofectamine 3000 (Invitrogen, Carlsbad, USA), respectively, to generate different types of recombinant lentivirus virions. NSCLC cells were infected with shRNA-expressing recombinant lentivirus and treated with 1 μ g/ml puromycin to generate CENPO-stably silencing cells. Fluorescence and infection efficiency were observed under microscope and the expression of CENPO were determined by Western blot.

Celigo cell counting assay

The cells were seeded in wells of 96-well plate (1000 cells/well \times 3 replicates for each group) at 37°C in an atmosphere of 5% CO₂. The Celigo Imaging Cytometer (Nexcelom, Lawrence, MA, USA) was used to calculate the living cells by measuring green fluorescence in each plate. The measurement began after 24 h incubation and daily measured for 5 days so that the cell growth curves were drawn.

Wound-healing assay

The cells were seeded in wells of 96-well plate at the density of 50,000 cell/well. After the 24h, cells were scratched with pipette tips, and the ablated cells were washed away with phosphate-buffered saline (PBS). According to the degree of wound-healing, the appropriate time was chosen to analyze the wound-healing area by cellomics (ArrayScan VT1, Thermo, USA). The mobility of the cells was determined by measuring the wound-healing area.

Transwell assay

Cell invasion ability was determined by Transwell assay, a Matrigel-coated modified Boyden chamber with a polycarbonate filter with a pore size of 8 μ m. 100 μ L cell suspensions (100,000~200,000 cell) with serum-free medium was added in the upper chamber of the transwell coated with 50 mg/ml of Matrigel solution. High-serum medium (30% FBS+1640) was then added to the lower chamber. After incubation for 24 h, the cells were fixed with a 4% formaldehyde solution for 30 mins and stained with giemsa solution. Five random fields in each chamber and photographed with a microscope at 100 \times magnification. ImagePro +6.0 was used to calculate the average migrated cells to determine the invasion capacity.

Flow cytometry (FCM)

The impact of CENPO expression on cell cycle and apoptosis was evaluated by flow cytometry (FCM) assay. The cells were seeded in wells of 6-well plate at 37°C in an atmosphere of 5% CO₂. When the cells grew to 80% confluence, they were collected by centrifugation at 1500 rpm for 5 min at 4°C and washed three times by cooled PBS solution. The cells were stained with propidium iodide (PI) (Sigma P4170) or

Annexin V (eBioscience) to determine cell cycle distribution and cellular apoptosis by flow cytometry using a Guava easy Cyte HT flow cytometer (Millipore).

Human Apoptosis Antibody Array analysis

Human Apoptosis Antibody Array (Abcam, Cambridge, MA, USA) was used to detect the effect of CENPO knockdown on the apoptosis pathway-related protein expression. NCI-H1299 cells infected with shCENPO were cleaved with 2 × cell lysis buffer. The membranes were incubated with 1.2 mL cell lysate overnight at 4°C, and then the liquid was discarded. Membranes were washed with 2 mL Wash Buffer I 3 times, and 2 mL Wash Buffer II 2 times, each time for 5 min. 1 mL 1 × Biotin-conjugated Anti-Cytokins were added and incubated with membranes overnight at 4°C. Wash Buffer I and Wash Buffer II were used to wash the membranes according to the above steps. The equal volume detection buffer C and detection buffer D were mixed evenly and added to the membranes for incubation for 2 min at room temperature. The signals were detected by chemiluminescence imaging system. And unpaired t-test was used for statistical analysis.

Nude mouse tumor formation model

Four-week old female BALB/c nude mice (Charles River Laboratories, Beijing, China) were divided into shCtrl (infected with shRNA control) and shCENPO (infected with CENPOsiRNA), 10 mice in each group. 2×10^6 cells were injected into each nude mice. Tumor sizes were measured every 5 days using a Vernier caliper. Tumor volume was calculated using the following formula: $\text{volume} = 0.5 \times \text{width}^2 \times \text{Length}$. After 39 days, the mice were sacrificed and were placed under the in vivo imaging system (LB983, Berthold Technologies) to observe the fluorescence. The tumors were removed from the mice, and then the weight of the tumors was measured. Tumor tissues were frozen in liquid nitrogen and stored at -80°C for further analysis.

Statistical analysis

Statistical analysis was carried out using SPSS software (version 21, SPSS Inc., Chicago, IL, USA). The data are presented as the mean ± S.E.M. Statistical analysis was performed with Student's t-test or one-way ANOVA, followed by Dunnett's test. All statistical tests were two-sided, and differences were considered to be significant at $P \leq 0.05$.

Results

Expression of CENPO in NSCLC tissues and cell-lines

The expression of CENPO in NSCLC tissues was firstly evaluated by UALCAN database. The transcriptional level of CENPO was upregulated in both LUAD (Figure 1A, $P < 0.001$) and LUSC (Figure 1E, $P < 0.001$) when compared with normal lung tissues. High CENPO expression was associated with lymphnode metastasis and advanced stage in both LUAD (Figure 1B and 1C) and LUSC (Figure 1F and

1G).Using the database of KM plotter, we found patient with higher CENPO was associated with worse overall survival (OS) in LUAD(HR=1.67, 95% CI=1.32-2.12, P=1.4×10⁻⁵, Figure 1D). However, no significant association was found in LUSC (P=0.35, Figure 1H).

The expression of 75 NSCLC and its corresponding adjacent normal lung tissues was examined by immunohistochemistry (IHC). The CENPO staining intensities in NSCLC was stronger than adjacent normal lung tissues (Figure 1I and 1J). According to the IRS=2, we divided the expression of CENPOas high expression (n=36) and low expression group (n=39). We found high CENPO was more frequently in patients with advanced stage (P<0.001, Table 1). However, no significant association was found between CENPO expression and OS in our clinical species (Figure 1K).Furthermore, the expression level of CENPO in NSCLC cell-lines was significant higher than normal lung epithelial cell-line EBC-1(P<0.05, Figure 1L).

Table 1. Relationship between CENPO expression and clinicopathologic characteristics in patients with NSCLC

| Features | No. of patients | CENPO expression | | p value |
|----------------------|-----------------|------------------|------|---------|
| | | low | high | |
| All patients | 75 | 39 | 36 | |
| Age (years) | | | | 0.100 |
| ≤62 | 39 | 17 | 22 | |
| >62 | 35 | 22 | 13 | |
| Gender | | | | 0.343 |
| Male | 69 | 37 | 32 | |
| Female | 6 | 2 | 4 | |
| Tumor size | | | | 0.132 |
| ≤5cm | 36 | 22 | 14 | |
| ≥5cm | 39 | 17 | 22 | |
| Lymph node positive | | | | 0.073 |
| =0 | 46 | 28 | 18 | |
| ≠0 | 28 | 11 | 17 | |
| Grade | | | | 0.247 |
| I | 2 | 1 | 1 | |
| II | 53 | 30 | 23 | |
| III | 20 | 8 | 12 | |
| Stage | | | | 0.001 |
| 1 | 28 | 21 | 7 | |
| 2 | 25 | 12 | 13 | |
| 3 | 22 | 6 | 16 | |
| T factor | | | | 0.220 |
| T1 | 7 | 3 | 4 | |
| T2 | 51 | 25 | 26 | |
| T3 | 16 | 10 | 6 | |
| T4 | 1 | 1 | 0 | |
| lymphatic metastasis | | | | 0.821 |

| | | | |
|----|----|----|----|
| N0 | 46 | 28 | 18 |
| N1 | 11 | 7 | 4 |
| N2 | 6 | 3 | 3 |

Establishment of CENPO knockdown cells

Three shRNAs were used to establishment of CENPO knockdown cells. The knockdown efficiency was confirmed by qRT-PCR (Additional file 1: Figure S1A, B). At last, shRNA3 was chosen because the knockdown efficacy was the highest among three shRNAs in NCI-H1299. After 72h, the transinfection efficacy of shRNA1 was observed under fluorescence microscope. As showed in Figure 2, it was demonstrates a >80% efficiency of infection and the normal cell condition (Figure 2A and 2D). Both qPCR and western blot suggested that transinfected with shCENPO significantly reduced CENPO mRNA and protein expression in both A549 (Figure 2B and 2C) and NCI-H1299 cell-lines (Figure 2E and 2F).

Reduced CENPO expression significantly inhibit cell proliferation, migration and invasive ability

Celigo cell counting assay was performed to evaluate the effect of CENPO on cell proliferation. We found that cells in shCENPO groups exhibit slower proliferation rate when compared with shCtrl groups in both A549 (Figure 3A) and NCI-H1299 (Figure 3B). Inwound healing assays, the observed time point of A549 was 24h and 72h (Figure 3C), but for NCI-H1299, it was 8h and 36h (Figure 3D). This was because the growth rate of two cell-lines was different. We found reduced CENPO dramatically suppressed the migration abilities of both cell-lines (Figure 3C and 3D). The invasion capability of A549 and NCI-H1299 transfected with shCENPO was evaluated by matrigel invasion chamber assay. As expected, reduced shCENPO groups notably repress the invasion ability when compared with shCtrl groups in both A549 (Figure 3E) and NCI-H1299 cell-lines (Figure 3F).

Reduced CENPO expression induced cell apoptosis and result in cell cycle arrest

In flow cytometry assay, Annexin-FITC positive cells in shCENPO groups were significantly increased when compared with shCtrl groups in both A549 (Figure 4A) and NCI-H1299 (Figure 4B). Cell cycle analysis showed reduced CENPO expression increased S and G2 cell population in A549. This increase in Sand G2–M phase cell population was accompanied with a concomitant decrease of cell number in G0/G1 phase in A549 (Figure 4C). In NCI-H1299, only increased G2 cell population accompanied with the decrease of G1 cell population was observed (Figure 4D).

Potential mechanism of CENPO in NCI-H1299

Firstly, Human Apoptosis Antibody Array analysis was applied to investigate the role of CENPO on apoptosis signaling pathway. We found reduced CENPO expression in NCI-H1299 result in the upregulation of BIM, Caspase3, IGF1R, p21 and the downregulation of IGF-II, Survivin, XIAP. (Figure 5A and 5B). Western blot was also performed to investigate the effect of CENPO on PI3K/Akt/mTOR and cell-cycle related protein mTOR, P-mTOR, CDK1, CDK6 and PIK3CA. In western blot analysis, we found H-1299

transinfected shCENPO reduced the expression of P-mTOR, CDK1, CDK6 and PIK3CA, no significant change was found in mTOR(Figure 5C).

Reduced CENPO inhibits NSCLC growth in vivo

To determine the effect of CENPO on tumor growth in vivo, male BALB/c nude mice were inoculated with NCI-H1299 transfected with shCENPO and shCtrl. Bioluminescent image of tumors suggested that the fluorescence intensity in mice with shCENPO was lower than shCtrl groups (Figure 6A and 6D). The tumor growth curves for mice was showed in Figure 6C, we found the tumor growth of shCENPO groups was slower than shCtrl groups. After the mice were sacrificed and tumors were

Removed, we found the tumor size of shCENPO groups was smaller than shCtrl group, what's more, no tumor were found in five mice in shCENPO group (Figure 6B), this was also agreed with the result of bioluminescent imaging. The tumor weight of shCENPO group was lighter than shCtrl group (Figure 6F). IHC staining of Ki67 was applied and confirmed that the expression of Ki-67 was suppressed in shCENPO group (Figure 6F). Taken together, Reduced CENPO inhibited tumorigenicity of NSCLC H1299 cell in nude mouse xenograft model

Discussion

The present study demonstrated that CENPO was up-regulated in NSCLC and was associated with unfavorable clinicopathologic feature such as TNM stage. Further in vitro and in vivo study demonstrated that reduced CENPO could attenuate the proliferation, migration and invasion ability of NSCLC cell-lines. Potential mechanism of CENPO in the progression of NSCLC was also explored; we found reduced CENPO attenuated malignant phenotype via promoted apoptosis signaling pathway, and affected PI3K/Akt/mTOR pathway and cell-cycle related proteins.

Firstly, the expression level of CENPO in NSCLC and its relationship between clinicopathologic feature was investigated by TCGA database and our clinical species from mRNA level and protein level. Both data suggested CENPO was frequently up-regulated in NSCLC when compared with normal lung tissues. Also, High CENPO expression was associated with malignant features such as TNM stage. However, the significant association between CENPO expression and OS was only found in LUAD from KM plotter. Further large sample size was necessary to verify the prognostic role of CENPO in NSCLC.

In vitro and in vivo study was further conducted to explore the role of CENPO in the progression of NSCLC. We found reduced CENPO inhibit the proliferation, migration and invasion ability of A549 and NCI-H1299. Reduced CENPO also induced apoptosis and result in cell cycle arrest. We found A549 and NCI-H1299 showed different biological behavior. NCI-H1299 growth more quickly than A549, as a result, in wound healing and assays, the observed time point of A549 was 24h and 72h, but for NCI-H1299, it was 8h and 36h. In cell cycle analysis, cell cycle arrest was happened in S and G2-M phase in A549, but in H1299, it was happened only in G2-M phase.

Further mechanism of CENPO in NSCLC was explored. Resisting Cell Death is a hallmark for cancer. Insufficient apoptosis was often observed in cancers(13). We investigated the effect of CENPO on apoptosis signaling pathway in NSCLC via Human Apoptosis Antibody Array. We found apoptosis signaling pathway related protein BIM, Caspase3, IGFBP-6 and p21 was upregulated and the IGF-II, Survivin and XIAP was downregulated in NCI-H1299 transfected with shCENPO. BIM was a proapoptotic BH3-only protein, and caspase-3 was apoptotic protein.(14) Up-regulation of BIM and caspase-3 induce apoptosis. Insulin-like growth factor (IGF) signaling also involved in apoptosis. (15) IGFBP-6 increased apoptosis was related to nuclear localization and interaction with transcription factors.(16) P21 exhibits anti-apoptotic activity owing to the inhibition of proteins involved in apoptosis. (17) Survivin, a member of the inhibitor of apoptosis protein(IAP) family that inhibits caspases and blocks cell death.(18) XIAP, a member of the IAP, has been identified as a potent caspase inhibitor. (19) Downregulated Survivin and XIAP promote apoptosis. As a result, reduced CENPO induced apoptosis via upregulated apoptosis promoting proteins and downregulated apoptosis inhibitor.

In addition, several PI3K/Akt/mTOR pathway and cell-cycle related protein (mTOR, P-mTOR, CDK1, CDK6 and PIK3CA) were detected by western blot. P-mTOR, CDK1, CDK6 and PIK3CA was downregulated when reduced CENPO expression. PI3K/Akt/mTOR pathway is known to be frequently activated in several types of cancer and it plays a critical role in a number of key cancerous behaviors. Both PIK3CA, mTOR and p-mTOR belonged to this pathway. The PIK3CA gene encodes p110 α , which is the catalytic subunit of PI3K, thus active PI3K-Akt signaling pathway. mTOR is a down-stream effector of PI3K-Akt signaling pathway. mTOR consists of two independent functional complexes, mTORC1 and mTORC2, which can be phosphorylated to p-mTOR regulating several cellular functions, including proliferation, differentiation, tumorigenesis, angiogenesis, autophagy, and apoptosis by activating ribosome biogenesis and protein synthesis.(20, 21) In our study, we found reduced CENPO expression would downregulate the expression of PIK3CA and p-mTOR, suggesting CENPO may activate PI3K/AKT/mTOR signaling pathway to promote cancer progression by avoiding apoptosis and other cellular behaviors.

Cyclin-dependent kinases (CDKs) are critical regulatory enzymes that drive all cell cycle transitions. CDK1 emerged as a key determinant of mitotic progression. In metazoans, much of the control over cell cycle entry is elicited at the level of CDK4 and CDK6, which are responsive to numerous growth regulatory signals. In the early phase of G1, the D-cyclins interact with CDK4/6 to form complexes to phosphorylate pRB, which is a tumor repressor required for transition from the G1 to S phase. CENPO belongs to Centromere protein, the deficiency of these proteins may affect the function of Centromere thus affected the cell cycle.(22) As previous studies reported, other Centromere protein such as CENPN knockdown (shCENPN) cells showed depressed cellular proliferation by cell-cycle arrest at the G1 phase with up-regulation of p21Cip1 and p27Kip1 and down-regulation of cyclin D1, CDK2, and CDK4.(23)

The mechanism of CENPO in cancer was insufficient, our research firstly demonstrated that CENPO may affect apoptosis related protein, cell cycle related proteins and PI3K/AKT/mTOR signaling thus regulated many malignant behaviors such as proliferation, apoptosis, cell cycle thus promoting the progression of NSCLC. However, whether these relationships had connected relationships or cross talking. As we know,

PI3K/AKT/mTOR signaling pathway may regulate apoptosis, cell cycle, is CENPO activated PI3K/AKT/mTOR signaling pathway then reduced apoptosis, cell cycle, or CENPO could be affected through them respectively, or through other pathways. And their direct binding site and detailed regulation, these problems should be investigated in the future.

Conclusion

In conclusion, our study suggested CENPO gene overexpression in NSCLC. Reduced CENPO expression substantially decreased the proliferation, migration and invasion ability, and promoting apoptosis and induces cell cycle arrest of NSCLC cell-lines. Preliminary mechanism research suggested reduced CENPO could activate apoptosis pathway, suppressing PI3K/AKT/mTOR pathway and down-regulation cell-cycle related proteins. Therefore, CENPO may be considered as an oncogene and it may be a new therapeutic target for the treatment of NSCLC. However, further studies, especially validation the prognostic role in larger clinical samples and explore the mechanism of CENPO were needed.

Abbreviations

CENPO: centromere protein O; NSCLC: non-small cell lung cancer; LUAD: lung adenocarcinoma; LUSC: lung squamous cell carcinoma; CCAN: centromere-associated network; OS: overall survival; IHC: Immunohistochemistry; FCM: Flow cytometry; IGF: insulin-like growth factor; IAP: inhibitor of apoptosis protein; CDKs: cyclin-dependent kinases.

Declarations

Ethics approval and consent to participate

Tissue microarray chips were purchased from Outdo Biotech, Ltd. (Shanghai, China). All the experiments and procedures of animals were performed in accordance with the National Institutes of Health guide for the care and use of Laboratory animals (NIH Publications No. 8023, revised 1978).

Consent for publication

Not applicable.

Availability of data and materials

All data generated or analyzed during this study are included in this published article.

Competing interests

The authors have no conflicts of interest to declare.

Funding

This study was supported by Scientific Research Foundation of Yunnan Education Department (2019J1234 and 2019J1282), Doctoral Research Foundation of the First Affiliated Hospital of Kunming Medical University (2018BS012) and Science and Technology Personnel Training Program of High-level Health Technicians in Yunnan Province (H-2017014).

Authors' contributions

Yunping Zhao: conception and design of the work. Yanlong Yang: conception, design of the work and have drafted the work. Xiaobo Chen: the acquisition, analysis. Hongwen Sun and Qinghe Yu: substantively revised. Fang Yin, Yongmeng Sun, Xinming Zhu, Shen Li, Zaoxiu Hu and Lisha Pu collected data and analyzed. All authors read and approved the final manuscript.

Acknowledgements

Not applicable.

References

1. Bray F, Ferlay J, Soerjomataram I, Siegel RL, Torre LA, Jemal A. Global cancer statistics 2018: GLOBOCAN estimates of incidence and mortality worldwide for 36 cancers in 185 countries. *CA Cancer J Clin.* 2018;68(6):394-424.
2. Feng RM, Zong YN, Cao SM, Xu RH. Current cancer situation in China: good or bad news from the 2018 Global Cancer Statistics? *Cancer Commun (Lond).* 2019;39(1):22.
3. Herbst RS, Morgensztern D, Boshoff C. The biology and management of non-small cell lung cancer. *Nature.* 2018;553(7689):446-54.
4. Yuen KW, Montpetit B, Hieter P. The kinetochore and cancer: what's the connection? *Curr Opin Cell Biol.* 2005;17(6):576-82.
5. Perpelescu M, Fukagawa T. The ABCs of CENPs. *Chromosoma.* 2011;120(5):425-46.
6. Okumura K, Kagawa N, Saito M, Yoshizawa Y, Munakata H, Isogai E, et al. CENP-R acts bilaterally as a tumor suppressor and as an oncogene in the two-stage skin carcinogenesis model. *Cancer Sci.* 2017;108(11):2142-8.
7. Kagawa N, Hori T, Hoki Y, Hosoya O, Tsutsui K, Saga Y, et al. The CENP-O complex requirement varies among different cell types. *Chromosome Res.* 2014;22(3):293-303.
8. Izuta H, Ikeno M, Suzuki N, Tomonaga T, Nozaki N, Obuse C, et al. Comprehensive analysis of the ICEN (Interphase Centromere Complex) components enriched in the CENP-A chromatin of human cells. *Genes Cells.* 2006;11(6):673-84.
9. Cao Y, Xiong J, Li Z, Zhang G, Tu Y, Wang L, et al. CENPO expression regulates gastric cancer cell proliferation and is associated with poor patient prognosis. *Mol Med Rep.* 2019;20(4):3661-70.

10. Chandrashekar DS, Bashel B, Balasubramanya SAH, Creighton CJ, Ponce-Rodriguez I, Chakravarthi B, et al. UALCAN: A Portal for Facilitating Tumor Subgroup Gene Expression and Survival Analyses. *Neoplasia*. 2017;19(8):649-58.
11. Gyorffy B, Surowiak P, Budczies J, Lanczky A. Online survival analysis software to assess the prognostic value of biomarkers using transcriptomic data in non-small-cell lung cancer. *PLoS One*. 2013;8(12):e82241.
12. Livak KJ, Schmittgen TD. Analysis of relative gene expression data using real-time quantitative PCR and the 2(-Delta Delta C(T)) Method. *Methods*. 2001;25(4):402-8.
13. Hanahan D, Weinberg RA. Hallmarks of cancer: the next generation. *Cell*. 2011;144(5):646-74.
14. Liu G, Pei F, Yang F, Li L, Amin AD, Liu S, et al. Role of Autophagy and Apoptosis in Non-Small-Cell Lung Cancer. *Int J Mol Sci*. 2017;18(2).
15. Baxter RC. IGF binding proteins in cancer: mechanistic and clinical insights. *Nat Rev Cancer*. 2014;14(5):329-41.
16. Bach LA, Fu P, Yang Z. Insulin-like growth factor-binding protein-6 and cancer. *Clin Sci (Lond)*. 2013;124(4):215-29.
17. Abbas T, Dutta A. p21 in cancer: intricate networks and multiple activities. *Nat Rev Cancer*. 2009;9(6):400-14.
18. Jaiswal PK, Goel A, Mittal RD. Survivin: A molecular biomarker in cancer. *Indian J Med Res*. 2015;141(4):389-97.
19. Devi GR. XIAP as target for therapeutic apoptosis in prostate cancer. *Drug News Perspect*. 2004;17(2):127-34.
20. Xu F, Na L, Li Y, Chen L. Roles of the PI3K/AKT/mTOR signalling pathways in neurodegenerative diseases and tumours. *Cell Biosci*. 2020;10:54.
21. Arafteh R, Samuels Y. PIK3CA in cancer: The past 30 years. *Semin Cancer Biol*. 2019;59:36-49.
22. Asghar U, Witkiewicz AK, Turner NC, Knudsen ES. The history and future of targeting cyclin-dependent kinases in cancer therapy. *Nat Rev Drug Discov*. 2015;14(2):130-46.
23. Oka N, Kasamatsu A, Endo-Sakamoto Y, Eizuka K, Wagai S, Koide-Ishida N, et al. Centromere Protein N Participates in Cellular Proliferation of Human Oral Cancer by Cell-Cycle Enhancement. *J Cancer*. 2019;10(16):3728-34.

Figures

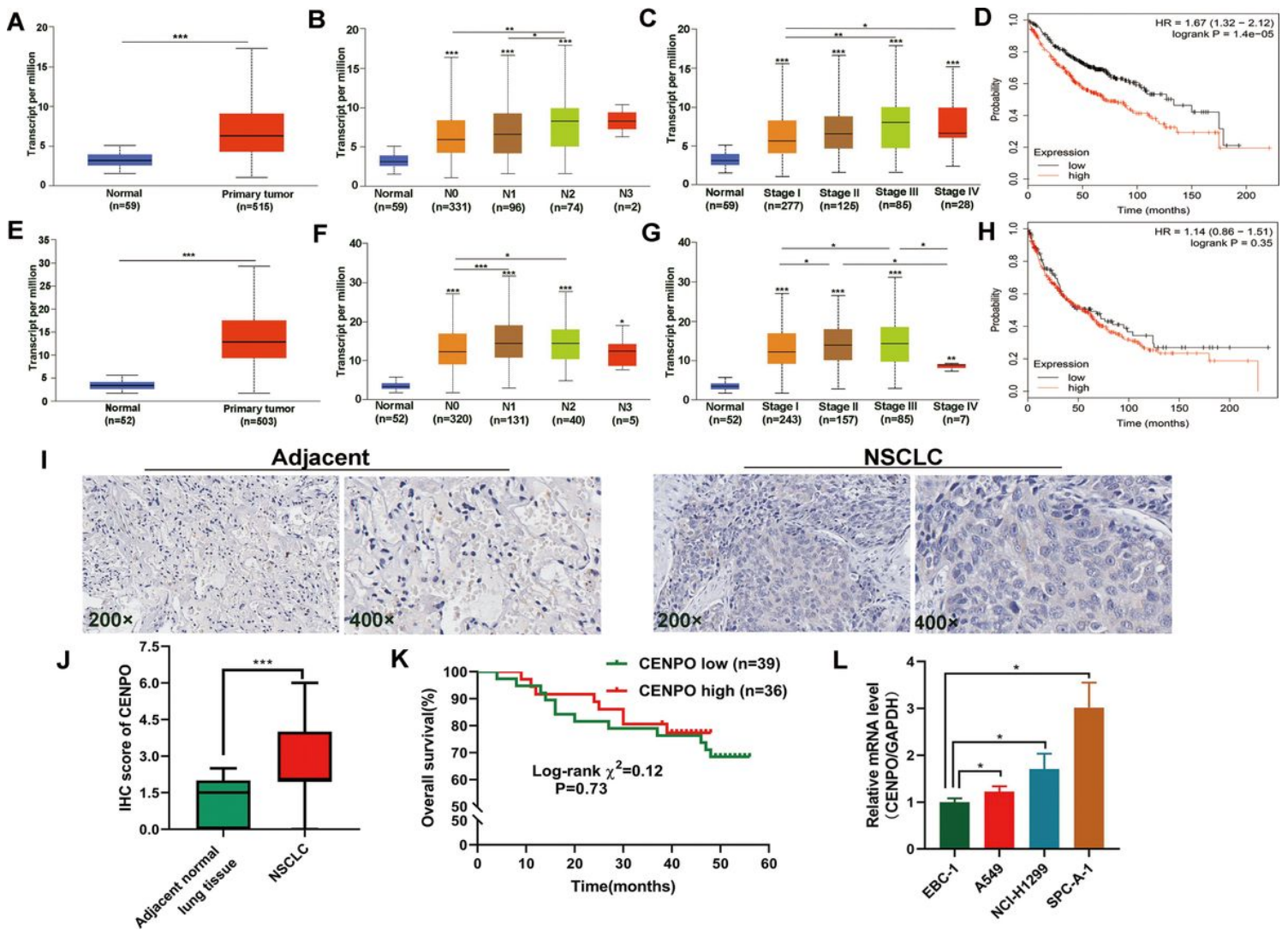


Figure 1

CENPO is highly expressed in NSCLC. A. Relative CENPO expression in lung adenocarcinoma (LUAD). And the association between CENPO expression and lymph node metastasis (B), tumor stage (C) and Overall survival (OS) of CENPO by Kaplan–Meier survival analysis (D) in LUAD. E. Relative CENPO expression in lung squamous cell carcinoma (LUSC). And the association between CENPO expression and lymph node metastasis (F), tumor stage (G) and OS of CENPO by Kaplan–Meier survival analysis (H) in LUSC. (The first layer asterisk which is right above the error bar representing comparison to normal group, and the above layers asterisk which were above a secondary line represent the comparison between corresponding groups that were covered by the line). I. Representative images with adjacent normal lung tissues and cancer tissues of IHC staining were shown. J The IHC score for CENPO staining was higher in NSCLC and normal lung tissues. K. Kaplan-Meier plotter was used to analyze the protein expression data from IHC. K. Relative CENPO mRNA expressions in normal human bronchial epithelial cells (EBC-1) and NSCLC cell lines (A549, H1299 and SPC-A-1). *P < 0.05, **P < 0.01, and ***P < 0.001.

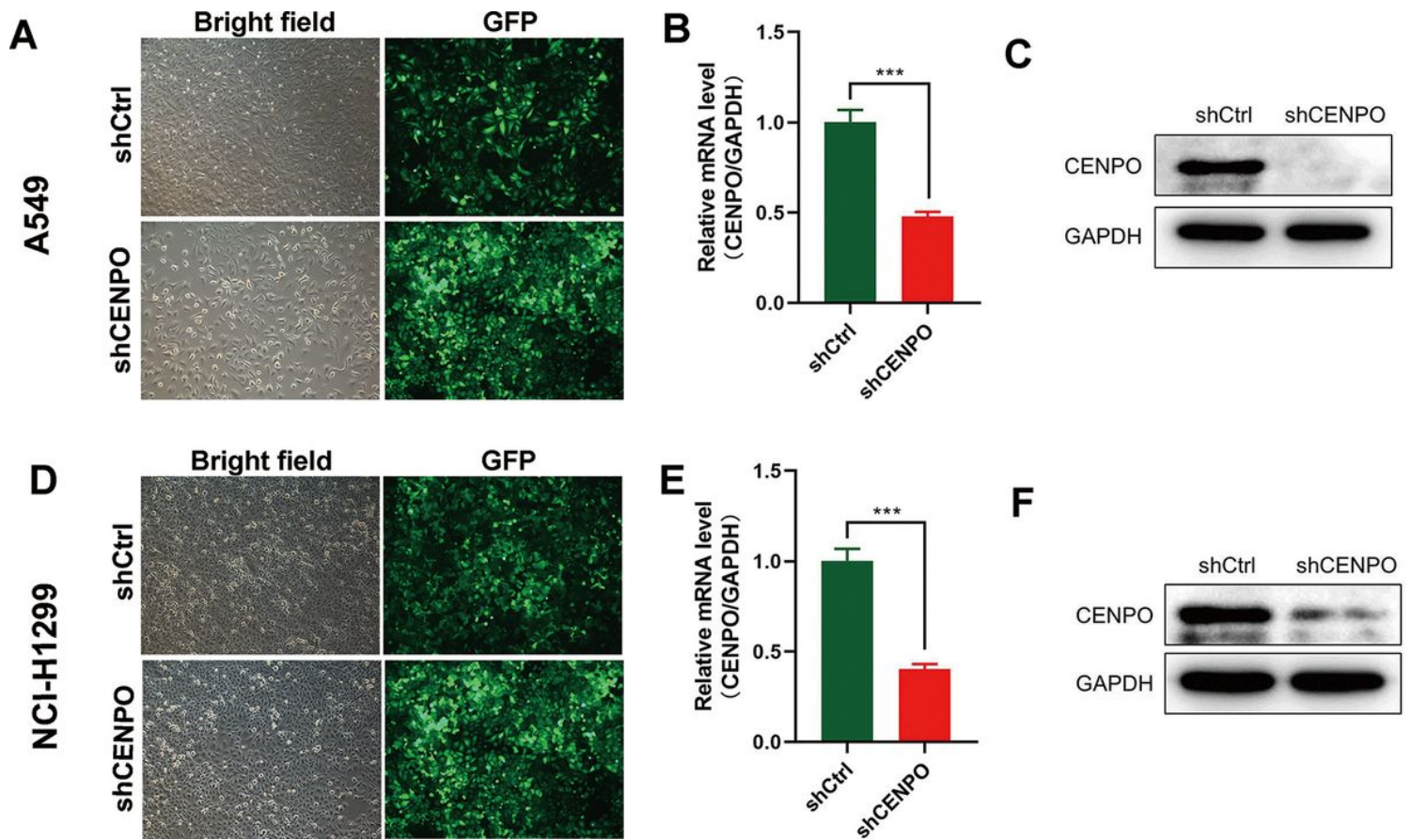


Figure 2

The transfection efficiency of CENPO knockdown. (A-C) The fluorescence expression of CENPO was observed under fluorescence microscope (A) and detected by qRT-PCR (B) and Western blot (C) in A549. (D-F) The fluorescence expression of CENPO was observed under fluorescence microscope (D) and detected by qRT-PCR (E) and Western blot (F) in NCI-H1299. *** $P < 0.001$.

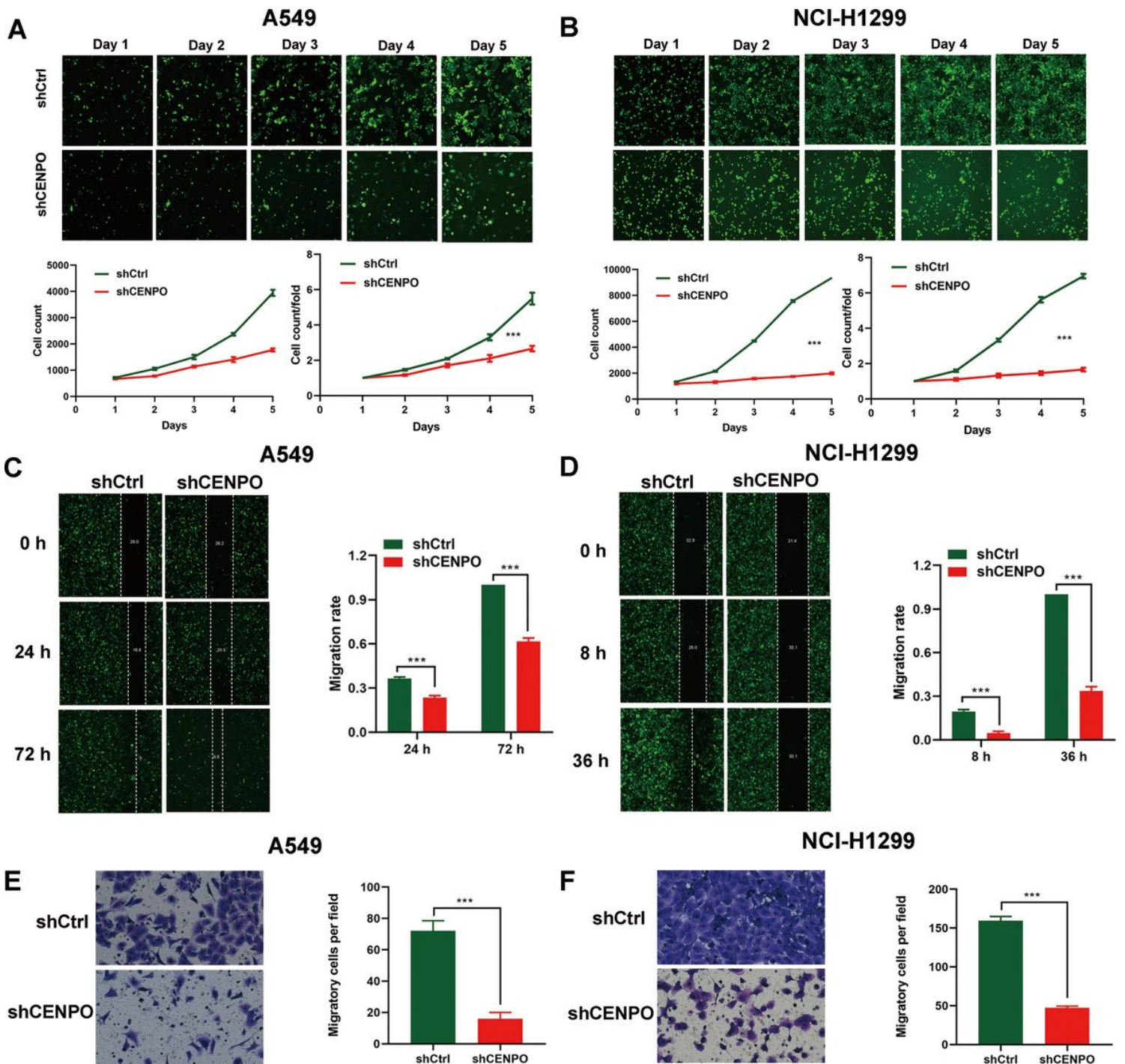


Figure 3

Reduced CENPO expression inhibited A549 and NCI-H1299 proliferation, migration and invasive ability. (A-B)The cell counting assay suggested reduced CENPO expression inhibited proliferation of A549 (A) and NCI-H1299 (B).(C-D)Wound healing assay suggested reduced CENPO inhibit the migration ability of A549 (C) and NCI-H1299 (D) cell-lines. (E-F)Transwell assay suggested reduced CENPO inhibit the invasiveability of A549 (E) and NCI-H1299 (F) cell-lines. ***P < 0.001.

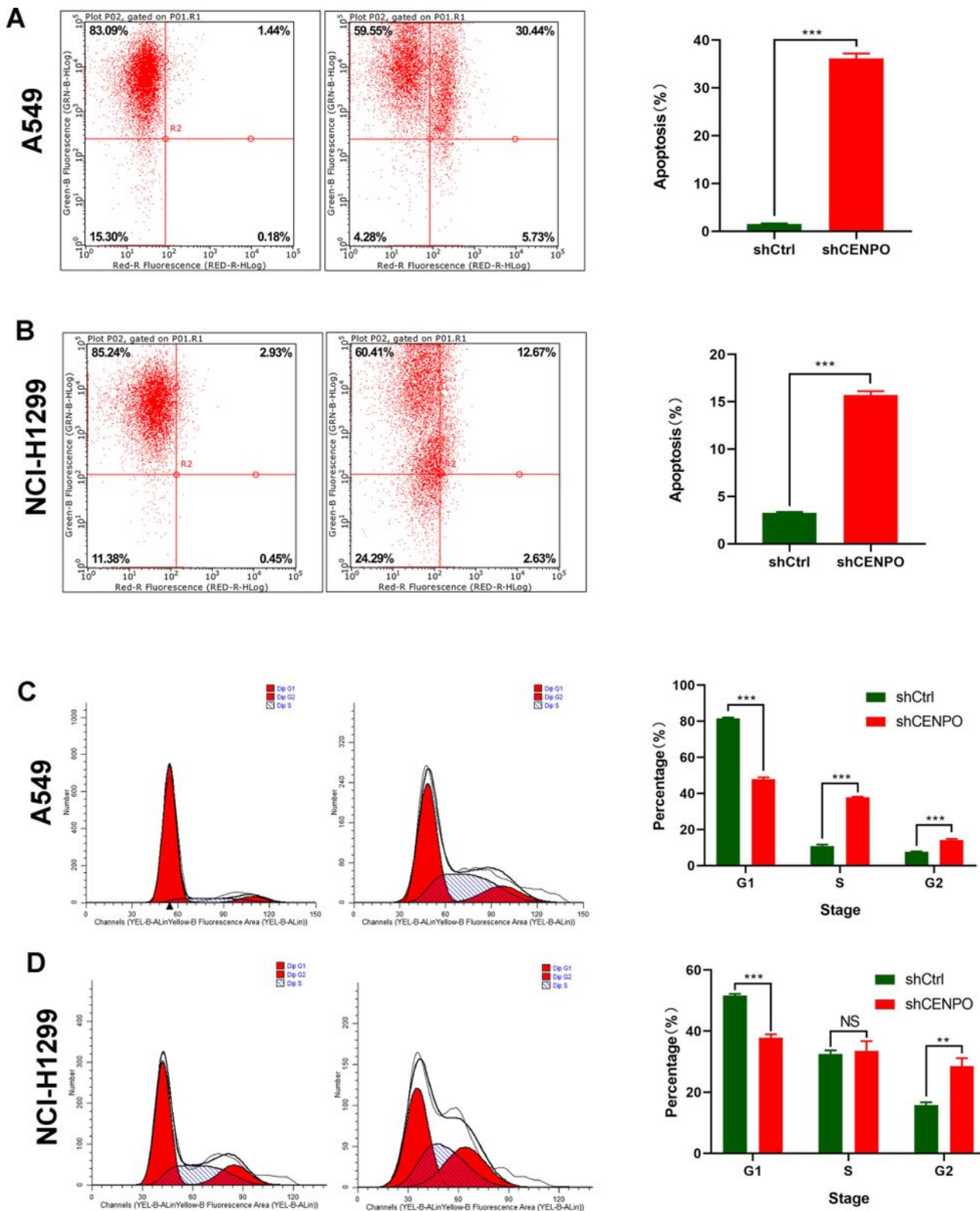


Figure 4

Flow cytometry suggested reduced CENPO expression induced cell cycle arrest and promote cellular apoptosis. (A-B) Reduced CENPO expression induced higher apoptosis rate in both A549 (A) and NCI-H1299 (B). (C-D) Reduced CENPO expression result in cell cycle arrest in both A549 (C) and NCI-H1299 (D). C. Increased S and G2 and decreased G1 cell population was observed in A549 transfected with

shCENPO. D. Increased G2 and decreased G1 cell population was observed in NCI-H1299 transfected with shCENPO. **P < 0.01, and ***P < 0.001.

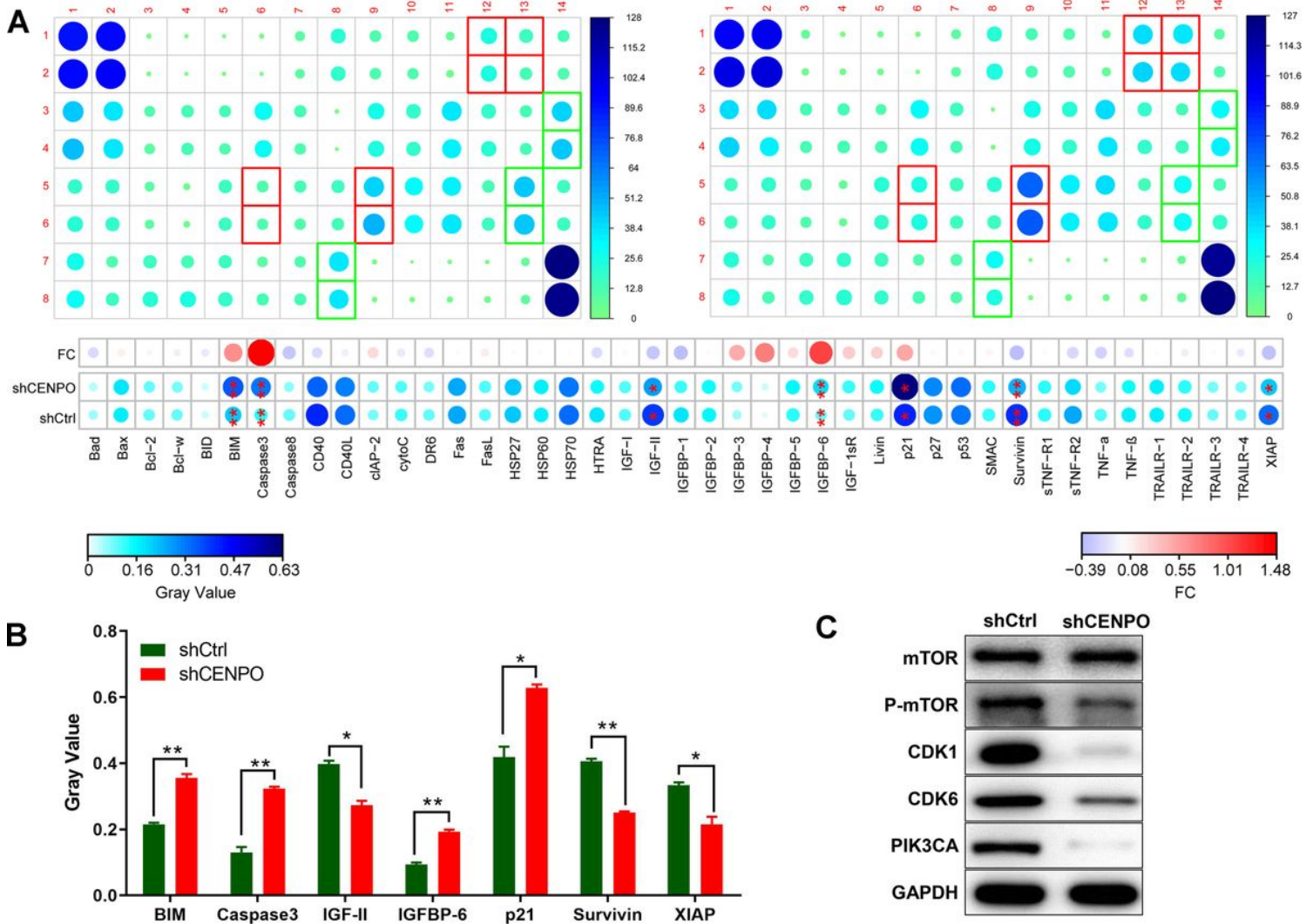


Figure 5

The intracellular molecular mechanism was investigated by HumanApoptosis Antibody Array and Western blot. (A) The expression of protein related with apoptosis signaling pathway in NCI-H1299 cells infected with shCENPO was measured by ECL with Human Apoptosis Antibody Array. (B) Reduced CENPO expression in NCI-H1299 result in the upregulation of BIM, Caspase3, IGFBP-6, p21 and the downregulation of IGF-I, Survivin and XIAP. (C) Western blot suggested NCI-H-1299 transfected shCENPO reduced the expression of P-mTOR, CDK1, CDK6 and PIK3CA, no significant change was found in mTOR

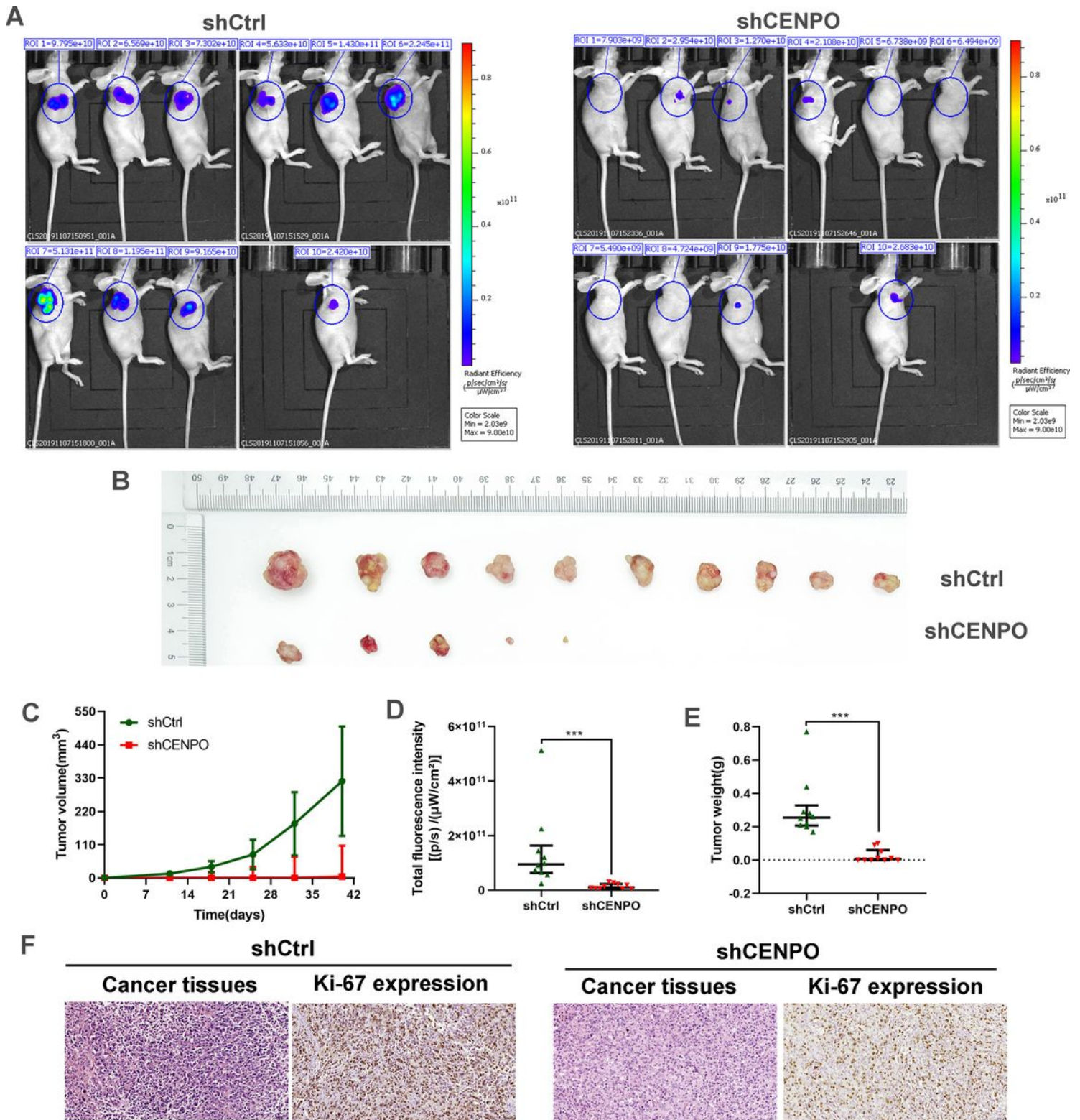


Figure 6

Reduced CENPO expression inhibited tumor growth in vivo. (A) The representative images of fluorescence image of mice models. (B) The representative images of solid tumors collected in mice. (C). Tumor volume was measured 6 times from feeding to sacrifice, and a broken line graph was recorded. (D) Total fluorescence intensity in vivo imaging of mice was detected (E) Tumor weight measured after mice

sacrificed. (F) The HE stain and Ki67 expression in mice model was detected by IHC staining. *** P < 0.001.

Supplementary Files

This is a list of supplementary files associated with this preprint. Click to download.

- [FigureS1.jpg](#)